Design and synthesis of amino-substituted *N*-arylpiperidinyl- -based inhibitors of the (immuno)proteasome

MARTINA GOBEC[1]
ALEŠ OBREZA[1]
MARKO JUKIČ[1,2]
ANA BAUMGARTNER[1]
ANJA MIHELČIČ[1]
ŠPELA POTOČNIK[1]
JULIJA VIRANT[1]
IRENA MLINARIČ RAŠČAN[1]
STANISLAV GOBEC[1]
IZIDOR SOSIČ[1,*] ⓘ

[1] *University of Ljubljana, Faculty of Pharmacy, 1000 Ljubljana, Slovenia*

[2] *Current address: University of Maribor, Faculty of Chemistry and Chemical Engineering, Laboratory of Physical Chemistry and Chemical Thermodynamics, 2000 Maribor Slovenia*

ABSTRACT

The constitutive proteasome and the immunoproteasome represent validated targets for pharmacological intervention in the context of various diseases, such as cancer, inflammation, and autoimmune diseases. The development of novel chemical scaffolds of non-peptidic nature, capable of inhibiting different catalytically active subunits of both isoforms, is a viable approach against these diseases. Such compounds are also useful as leads for the development of biochemical probes that enable the studies of the roles of both isoforms in various biological contexts. Here, we present a ligand-based computational design of (immuno)proteasome inhibitors, which resulted in the amino-substituted *N*-arylpiperidine-based compounds that can inhibit different subunits of the (immuno)proteasome in the low micromolar range. The compounds represent a useful starting point for further structure-activity relationship studies that will, hopefully, lead to non-peptidic compounds that could be used in pharmacological and biochemical studies of both proteasomes.

Keywords: proteasomes, scaffold morphing, optimization, computational design, selectivity, inhibitors

All intracellular and many extracellular proteins undergo continuous degradation and resynthesis. Eukaryotic cells contain several proteolytic systems and complex mechanisms, which ensure that the degradation process is strictly regulated. Extracellular and membrane proteins are mainly degraded in lysosomes by endocytosis, phagocytosis or pinocytosis. On the other hand, most intracellular proteins are degraded *via* the ubiquitin--proteasome system (UPS). The 26S proteasome is the principal proteolytic machine within the UPS and plays a key role, including the rapid degradation of misfolded and damaged proteins and the slower degradation of most other intracellular proteins (1, 2). The 26S proteasome is therefore essential for protein homeostasis and during the past two decades, a critical role for the UPS has been established in essentially every process inside cells, including immune response, cell cycle progression, regulation of transcription, genome integrity, and apoptosis (3–7).

---

* Correspondence; e-mails: izidor.sosic@ffa.uni-lj.si

The 26S proteasome is a large multicatalytic complex (see below) that breaks down ubiquitin-tagged proteins. Ubiquitin is a small protein, consisting of 76 amino acids, and its attachment to the target protein represents a signal for proteasome processing and degradation. This process involves three sequentially-acting enzymes: E1 (ubiquitin-activating enzyme), E2 (ubiquitin-conjugating enzyme), and E3 (ubiquitin ligase). Ubiquitination begins with the activation of ubiquitin *via* the activating enzyme E1 in an ATP-dependent reaction. The terminal carboxyl group of ubiquitin binds *via* the thioester bond to the cysteine residue of E1. Ubiquitin is then transferred to one of the isoforms of the E2 conjugation enzyme. The key enzymes throughout the process, however, are the ubiquitin E3 ligases, because they recognize specific protein substrates and catalyze the transfer of activated ubiquitin from E2 to the targeted proteins (8–10). The C-terminal glycine residue of activated ubiquitin binds covalently to the side NH_2 group of the lysine on the substrate *via* an iso-peptide bond. By sequentially adding more ubiquitin molecules to the same protein, a poly-ubiquitin chain is synthesized. At least four ubiquitin molecules must be bound to the protein for proteasome tagging. The labeled proteins then bind to the 19S regulatory domain of the 26S proteasome, where they are deubiquitinated and unfolded (4). The unfolded proteins enter the catalytic part of the machinery (20S proteasome or core particle), where they are cleaved into peptides containing from 3 to 22 amino acids. The peptides are then released together with free ubiquitin (which is recycled) and are further degraded by cytosolic amino and carboxypeptidases, and a small fraction of the peptides are transferred to endoplasmic reticulum membranes, where they bind to major histocompatibility complex class I molecules and are presented to cytotoxic T cells that trigger an immune response (11, 12).

The 26S proteasome, in its constitutive form, comprises a 20S core particle (CP) that is flanked by regulatory 19S moieties on both ends (Fig. 1). The CP, a 720 kDa barrel-shaped structure, consists of four stacked rings: two outer α-rings and two inner β-rings, each composed of seven subunits. While the outer α-rings contribute to the protein's structural integrity and create a passage for substrate entry, they lack catalytic activity. On the other hand, the inner β-rings possess proteolytic functions (13, 14). Each ring contains three subunits with catalytic activity, responsible for protein breakdown. The β5 subunit (chymotrypsin-like) cleaves bonds following hydrophobic residues, the β1 subunit (caspase-like) cleaves peptide bonds after acidic residues, and the β2 subunit (trypsin-like) cleaves bonds after basic residues (Fig. 1) (15).

In vertebrates, three types of CPs are known. Namely, the constitutive proteasome (cCP) found in all cells, the thymoproteasome, which is found only in the epithelial cells of the thymus cortex, and the immunoproteasome (iCP) expressed mainly in cells of the hematopoietic origin, such as the lymph nodes, spleen, and bone marrow. In non-hematopoietic cells exposed to inflammatory factors, such as tumor necrosis factor α and interferon-γ, the synthesis of iCP active subunits β (designated as β1i, β2i, β5i), which replace their constitutive counterparts is induced (12, 17). In addition, the regulatory 19S part is replaced by the regulatory 11S part (Fig. 1) (18). Unlike cCP, iCP has markedly decreased caspase-like activity and increased chymotrypsin- and trypsin-like proteolytic activities. Consequently, iCP has a higher affinity for the cleavage of peptides with hydrophobic and basic residues. This results in the production of peptide fragments optimized for binding to MHC class I molecules and presentation to cytotoxic T-cells, leading to the initiation of an immune response (12).

Disruption of the UPS that is caused by either increased expression of both proteasomes or their activities can lead to a number of diseases. These include many types of
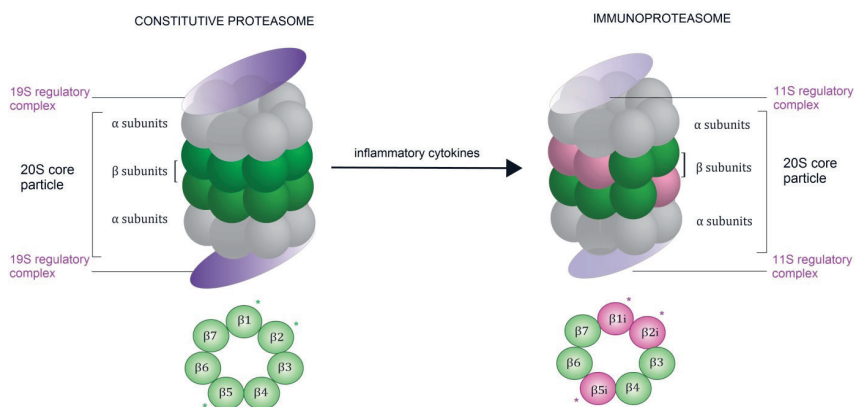
Fig. 1. Schematic representations of the constitutive proteasome and the immunoproteasome. Under the influence of inflammatory conditions, the expression of immuno-subunits β1i, β2i, and β5i is induced. Green and violet stars denote catalytically-active subunits of the constitutive proteasome and the immunoproteasome, resp. Figure adapted from ref. 16.

cancer, infections, inflammatory and autoimmune diseases (Crohn's disease, ulcerative colitis, hepatitis, and rheumatoid arthritis), as well as neurological disorders (19–23). Hence, the cCP and the iCP are deemed valid targets for the design of new biologically relevant compounds (24–31). Our lab recently reported on reversible and irreversible non-peptidic inhibitors of the β5i subunit of the human iCP with inhibitory activities in the low micromolar and nanomolar range, resp. (32–34). These compounds were also able to discriminate between the iCP and the cCP *in cellulo*. With the aim to expand the chemical space of non-peptidic iCP and cCP inhibitors, the current study was focused on a computationally-driven scaffold morphing approach to replace the large central psoralen ring with novel ring systems. This approach led to the discovery of novel, yet simplified compounds, which were prepared *via* a straightforward three-step synthesis. The initial biochemical evaluation was focused on inhibition assays on the β5i subunit of the iCP, followed by assays of the most potent compounds for inhibitory activities on the remaining subunits of both proteasomes to determine their selectivities. These efforts resulted in several amino-substituted *N*-arylpiperidinyl-based inhibitors with inhibition of different iCP and cCP subunits in the low micromolar range.

EXPERIMENTAL

General chemistry

Chemicals from commercial sources (Sigma Aldrich, USA, Fluorochem, UK, TCI, Japan, Apollo Scientific, UK, Enamine, Ukraine) were used without further purification. Anhydrous THF, DCM, and Et_3N were dried and purified by distillation over Na, K_2CO_3, and KOH, resp. Analytical thin-layer chromatography (TLC) was performed on Merck silica gel ($60F_{254}$) plates (0.25 mm). Flash column chromatography was performed on Silica gel 60 (Merck, Germany, particle size 0.040–0.063 mm). The mobile phases are reported for each individual synthetic step.

^{1}H and ^{13}C NMR spectra were recorded on a Bruker AVANCE III 400 (USA) spectrometer at 295 K in CDCl$_3$ or DMSO-d_6 solutions with TMS as the internal standard. The chemical shifts (δ) are reported in parts per million (ppm) downfield from TMS. All the coupling constants (J) are reported in hertz (Hz). IR spectra were recorded on a PerkinElmer Spectrum BX System FT-IR spectrometer (USA). Mass spectra were measured with an Advion expression CMLS mass spectrometer with ESI ionization (USA). High-resolution mass spectra were obtained with the ExactiveTM Plus Orbitrap Mass Spectrometer with ESI ionization (ThermoFisher Scientific, USA).

Melting points were determined on a Reichelt hot-stage and are uncorrected. All reported yields are yields of purified products.

Analytical reversed-phase HPLC for the test compounds was performed on a Thermo Scientific DIONEX UltiMate 3000 instrument (USA) equipped with a diode array detector using Kromasil 5-CelluCoat normal-phase column (10 × 250 mm, 5 μm), which was thermostated at 25 °C, with a flow rate of 4.0 mL min^{-1} and a sample injection volume of 10 μL. An eluent system of *n*-hexane (from 70 to 85 %) and EtOH (from 30 to 15 %) was used, depending on the characteristics of the compound analyzed. The purities of all assayed compounds used for the biological evaluations were > 95 %, as determined by HPLC.

Computational research

General information on computational hardware. – The compound database preparation and all of the computations were carried out on a four eight-core AMD Opteron 6128 Magny-Cours workstation with 32 GB RAM, 4 × 1 TB HDD, running 64-bit Ubuntu Linux 18.04. Experiment analysis was conducted on a two quad-core Intel Xeon 2.2 GHz workstation with 16 GB RAM, 1 TB HDD, 1 TB SSD, and an Nvidia GTX 1050 graphic card, running 64-bit Debian Linux (Sparky) and on a workstation with 8-core Intel i7 Haswell 4710, 2.5 GHz processor running Microsoft Windows 10 operating system.

Computational design of compounds. – The parameters used for a screening fragment database were as follows: -smarts all; -capAttach true; -flipper 5; -forceFlip false; -flipN true; -omega true; -readConfs (not set, no default); -primaryFrag false; -filter true: -minFrequency 0; -minDegree 1; -maxDegree 3; -maxMolWt 350.0; -minHvy 0; -maxHvy 15; -maxChiral 3. The employed CHOMP filter was defined as: MAX_MOLWT 900; ELIMINATE_METALS Sc, Ti, V, Cr, Mn, Fe, Co, Ni, Cu, Zn, Y, Zr, Nb, Mo, Tc, Ru, Rh, Pd, Ag, Cd and defined ALLOWED_ELEMENTS H, C, N, O, F, S, Cl, Br, I.

The vBROOD parameters used were as follows: -bondOrder true, -attachmentCutoff 0.78, -shapeCutoff 0.6, -attachmentScale 1.5, -checkGeometry true, -fromCT false, -fileChrg false, -interval 5000, -hitinterval 1000, -rangeSize 6, -rangeOffset, -bumpRadius 2.25 and -forcefield MMFF94S.

The parameters for the filtering step with a 'Drug-like' filter in BROOD were as follows: Heavy Atom Count ≤ 35, Molecular Weight ≤ 500, Rotor Count ≤ 13, LogP ≤ 5.0, Polar Surface Area ≤ 150, Lipinski Donor Count ≤ 5, Lipinski Acceptor Count ≤ 10, Lipinski Failures ≤ 2, ABS ≥ .25, Fraction sp^3 Carbons ≥ 0.3)

Residual activity measurements

This assay was performed as described previously (32). Briefly, the preliminary screening of compounds was performed at 100 μmol L^{-1} final concentrations in the assay

buffer (0.01 % SDS, 50 mmol L^{-1} Tris-HCl, 0.5 mmol L^{-1} EDTA, pH 7.4. To 50 µL of each compound, 25 µL 0.8 nmol L^{-1} human iCP (Boston Biochem, Inc., USA) was added. After 30 min incubation at 37 °C, the reaction was initiated by the addition of 25 µL 100 µmol L^{-1} succinyl-Leu-Leu-Val-Tyr-7-amino-4-methylcoumarin (Suc-LLVY-AMC) (Bachem, Switzerland) (final concentration was 25 µmol L^{-1}). The reaction progress was recorded on the BioTek Synergy HT microplate reader by monitoring fluorescence at 460 nm (λ_{ex} = 360 nm) for 90 min at 37 °C. The initial linear ranges were used to calculate the velocity and to determine the residual activity.

Determination of IC_{50} *values*

This assay was performed as described previously (32). Briefly, the final assay mixtures contained 0.2 nmol L^{-1} human iCP or 0.8 nmol L^{-1} human cCP (both from Boston Biochem) in the assay buffer (0.01 % SDS, 50 mmol L^{-1} Tris-HCl, 0.5 mmol L^{-1} EDTA, pH 7.4). Inhibitors were dissolved in DMSO and added to black 96-well plates for at least eight different concentrations (the final concentration of DMSO did not exceed 1 %). In the case of the β2 activity inhibition determination, the assay buffer was modified; SDS was replaced with the proteasomal activator PA28α (Boston Biochem). After 30 min of incubation at 37 °C, the reaction was initiated by the addition of the relevant fluorogenic substrate: Suc-LLVY-AMC for β5i and β5, *t*-butyloxycarbonyl-Leu-Arg-Arg-7-amino-4-methylcoumarin (Boc-LRR-AMC) for β2i and β2, benzyloxycarbonyl-Leu-Leu-Glu-7-amino-4-methylcoumarin (Z-LLE-AMC) for β1 (all from Bachem), and acetyl-Pro-Ala-Leu-7-amino-4-methylcoumarin (Ac-PAL-AMC) for β1i (Boston Biochem). The fluorescence was monitored at 460 nm (λ_{ex} = 360 nm) for 90 min at 37 °C. The progress of the reactions was recorded and the initial linear ranges were used to calculate the velocity. IC_{50} values were calculated in Prism (GraphPad Software, CA, USA) and are means from at least three independent determinations. To determine the IC_{50} shift for compound *N*-((1-(4-morpholinobenzyl)piperidin-4-yl)methyl)acrylamide (**10e**) on the β5 and the β5i subunits (see Table III in the RESULTS AND DISCUSSION), the same protocol was used, except for the 0 min of incubation timer prior to the addition of the substrate Suc-LLVY-AMC.

RESULTS AND DISCUSSION

Computational-based design

As the initial step in compound design, we prepared a screening fragment database using ChEMBL 20 open large-scale bioactivity database of drug-like compounds as a structure library, Drugbank database, and CHOMP (Chemical heuristic for optimal molecular pieces) software from OpenEye (version 3.0.0.3; OpenEye Scientific Software Inc., Santa Fe, New Mexico). The final library consisted of 5 923 570 fragments from CheEMBL and 307 178 fragments from Drugbank (35) (Fig. 2). For the details on parameters used in this step of *in silico* design, see EXPERIMENTAL.

Second, the parent psoralen-based structure was fragmented in order to isolate the central psoralen scaffold and leave the decoration handles (substituents) intact. After psoralen (M_r = 333, XLog*P* = 3.9, 2D PSA = 83, rotor count = 3, 25 heavy atoms) fragmentation and disconnection across two bonds, the central psoralen core was chosen as a query for
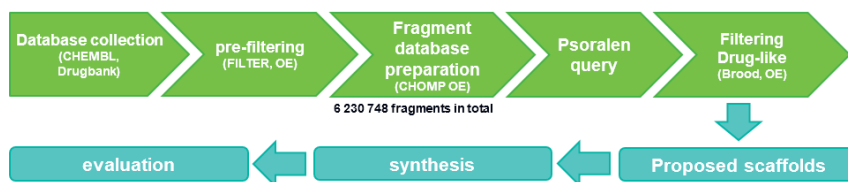
Fig. 2. *In silico* design protocol for the identification of novel amino-substituted *N*-arylpiperidinyl--based inhibitors of the iCP.

bioisosteric replacement using BROOD/vBROOD software from OpenEye (version 3.0.0.3; OpenEye Scientific Software Inc., USA) (Fig. 2). BROOD/vBROOD was utilized, because this software enables comparison of the sterical similarity, chemical connectivity of library fragments, and electrostatic similarity to the initial query structure with NEAT (Novel and electronically-equivalent aromatic template) that uses pre-calculated quantum mechanical charges to search for aromatic rings with similar electrostatic potentials, dipoles, and hydrogen bonding capabilities to the query template (36, 37). The filtering step with a 'drug-like' filter in BROOD search, in which fragments are filtered based on values obtained by removing the query contribution, was also employed (Fig. 2).

This *in silico* screening protocol resulted in 3- or 4-substituted amino- and amino-methyl-piperidine scaffolds as the highest-ranking hits (*e.g.,* nipecotamide; M_r = 309.41, XLog$P$ = 2.42, 2D PSA = 59.22, rotor count = 4, 23 heavy atoms with combo tanimoto similarity score of 1.46; vBROOD OpenEye) (Fig. 3, general structure in the middle). These
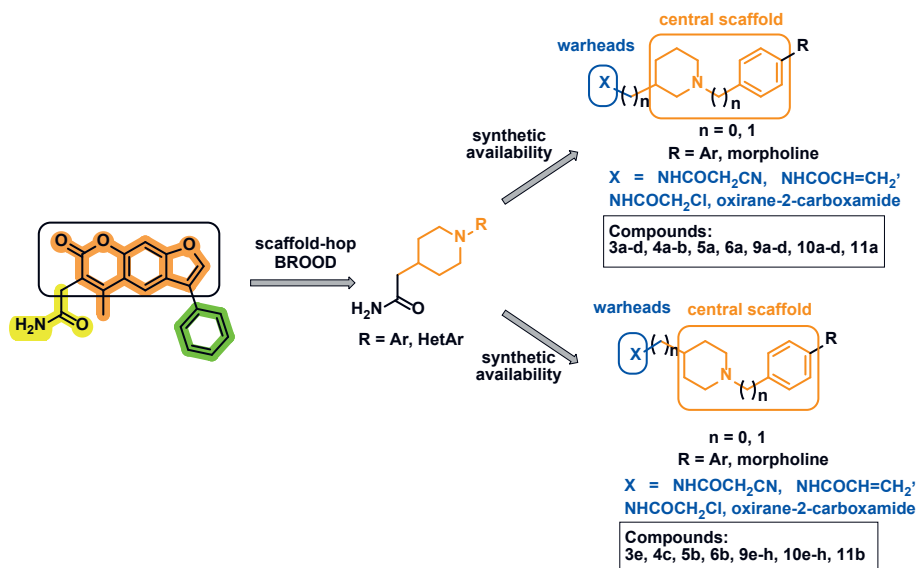
Fig. 3. Simplified representation of the computational design that yielded 3- or 4-substituted amino- and aminomethyl-piperidines, additionally modified with phenyl or benzyl moiety at position 1. The general structures of the two classes are shown.

identified moieties were then selected as starting points for the evaluation of the synthetic availability of a central scaffold that could be highly modifiable and could additionally enable the incorporation of various electrophilic warheads at positions 3 or 4 at the piperidine ring. The decision to incorporate electrophilic moieties into the newly designed molecules was based on our previous work (32–34), where such medicinal chemistry approach yielded very potent, irreversible, and subunit-selective compounds. Of note, most advanced inhibitors of (immuno)proteasomes possess strongly (*e.g.*, epoxyketones, acrylamides, oxathiazol-2-ones) or mildly (*e.g.*, boronic acids) electrophilic fragments (24, 30) that react with the catalytic Thr in iCP and cCP active sites.

Synthesis

The initial preparation of simple *N*-benzyl-substituted piperidin-3-yl-oxathiazol-2-ones and their biochemical evaluation resulted in only moderate inhibitory activity of the β5i subunit (38). This preliminary information was important in terms of design because we realized that elongation of the central scaffold (Fig. 3, structures in orange squares) was needed to better mimic the parent psoralen-based compound (Fig. 3, left structure). Therefore, we first synthesized a library of 3- or 4-substituted *N*-[1,1'-biphenyl]-4-carbonylpiperidines and 3- or 4-substituted *N*-[1,1'-biphenyl]-4-methylenepiperidines with different electrophilic groups attached at positions 3 or 4 (compounds **3–6**, Scheme 1; for exact structures of compounds, please refer to Table I), which corresponded better to the general
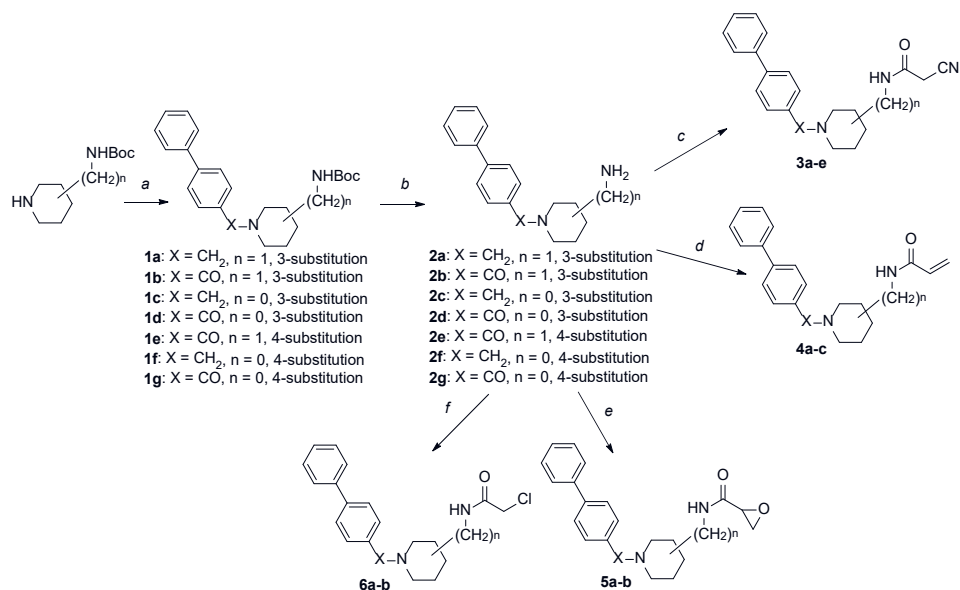
Scheme 1. Reagents and conditions: (a) [1,1'-biphenyl]-4-carbaldehyde, NaCNBH$_3$, THF or [1,1'-biphenyl]-4-carbonyl chloride, *N*-methylmorpholine, CH$_2$Cl$_2$; (b) CF$_3$COOH, CH$_2$Cl$_2$; (c) cyanoacetic acid, HOBt, EDC, DIPEA, CH$_2$Cl$_2$; (d) acryloyl chloride, DIPEA, CH$_2$Cl$_2$; (e) potassium oxirane-2-carboxylate, HOBt, EDC, *N*-methylmorpholine, DMF; (f) chloroacetyl chloride, DIPEA, CH$_2$Cl$_2$.
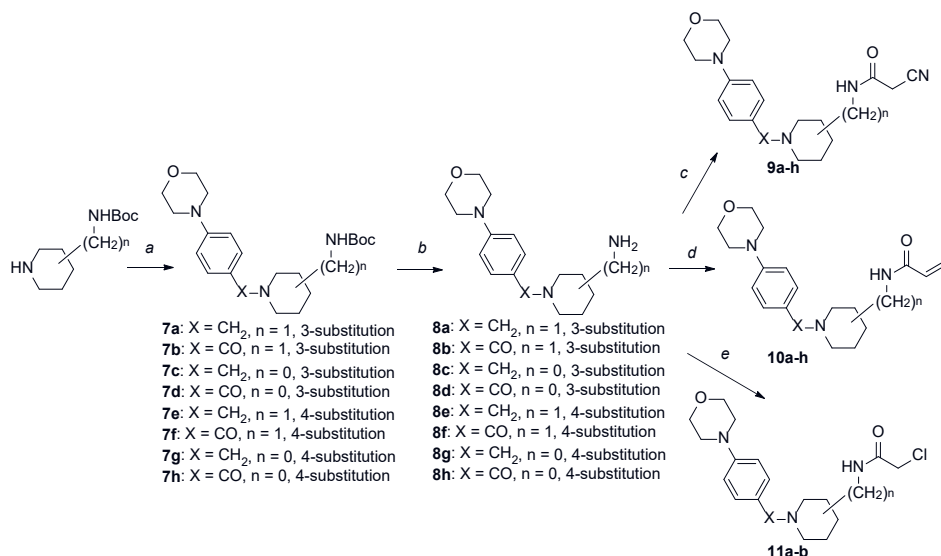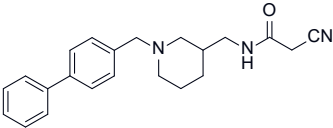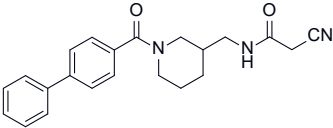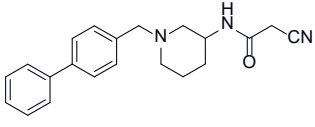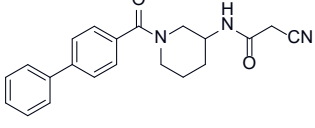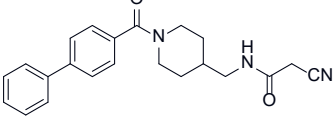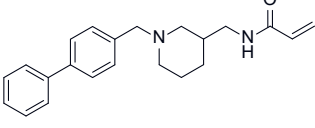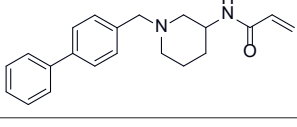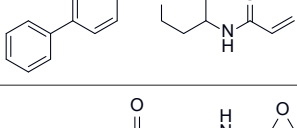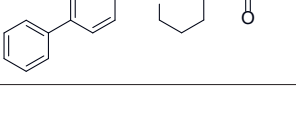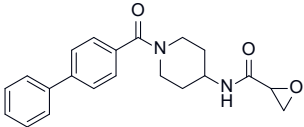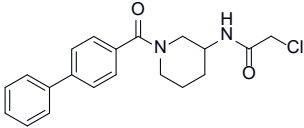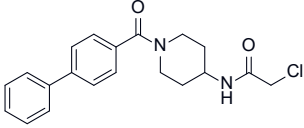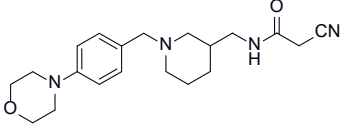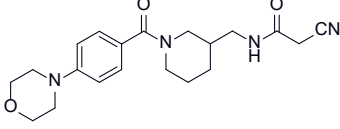
Scheme 2. Reagents and conditions: (a) [1,1'-biphenyl]-4-carbaldehyde, NaCNBH$_3$, THF or [1,1'-biphenyl]-4-carbonyl chloride, *N*-methylmorpholine, CH$_2$Cl$_2$; (b) CF$_3$COOH, CH$_2$Cl$_2$; (c) cyanoacetic acid, HOBt, EDC, DIPEA, CH$_2$Cl$_2$; (d) acryloyl chloride, DIPEA, CH$_2$Cl$_2$; (e) chloroacetyl chloride, DIPEA, CH$_2$Cl$_2$.

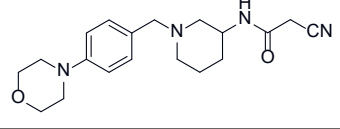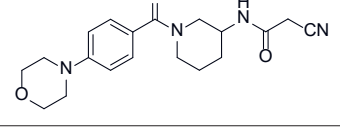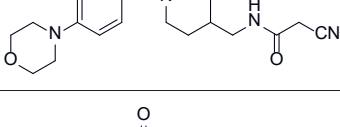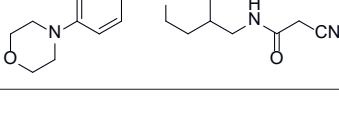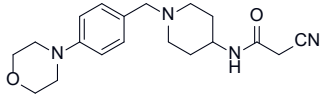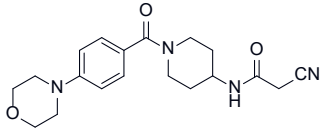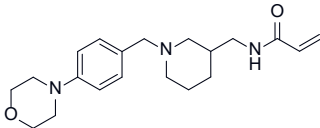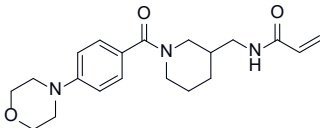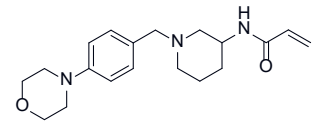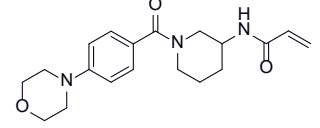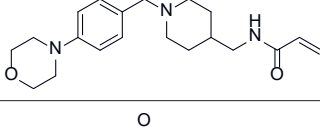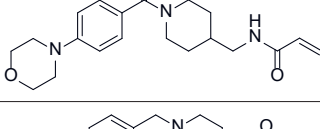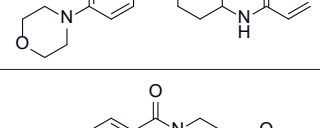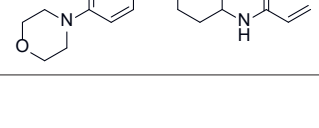structures in Fig. 3 (structures on the right-hand side). Please note that the detailed synthetic procedures and spectroscopic analyses of all intermediates and final compounds, described in Scheme 1, are available in the Supplementary data.
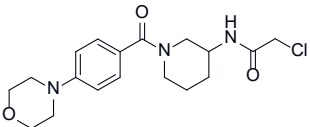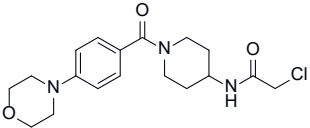
The synthesis of biphenyl derivatives **3–6** (Scheme 1) started with the acylation (using [1,1'-biphenyl]-4-carbonyl chloride) or reductive amination (using [1,1'-biphenyl]-4-carbaldehyde) of commercially available Boc-protected amino- and aminomethyl-piperidines. The TFA-mediated deprotection of the primary amino group of compound **1** was followed by coupling of the free amines **2** with corresponding carboxylic acids or acyl halogenides to introduce various electrophilic warheads and to obtain cyanoacetamides **3**, acrylamides **4**, oxirane-2-carboxamides **5**, and chloroacetamides **6**. To further explore the structure-activity relationship (SAR), increase solubility, reduce the number of aromatic rings, and consequently increase the drug-likeness of final compounds (39), we decided to replace one of the aryl groups from a previous series of compounds (*i.e.*, **3–6**) with morpholine. Despite this modification, we retained the design and substitution patterns as established by the computational design (Fig. 3, structures on the right-hand side). The synthetic pathway towards envisaged compounds is presented in Scheme 2 (for exact structures of compounds, please refer to Table I). Here, 4-morpholinobenzaldehyde and 4-morpholinobenzoyl chloride were used to prepare Boc-protected derivatives **7**, which were subsequently deprotected using TFA to yield amino- and aminomethyl-piperidines **8**. These were then converted by coupling reactions into cyanoacetamide derivatives **9**, acrylamides **10,** and chloroacetamides **11**. Please note that the detailed synthetic procedures and spectroscopic analyses of all intermediates and final compounds, described in Scheme 2, are available in the Supplementary data.

Table I. Inhibitory potencies of compounds against the β5i subunit of human iCP[a]

Compd.	Structural formula	RA or IC_{50}[b]
3a		3 %[c]
3b		100 %
3c		100 %
3d		100 %
3e		100 %
4a		95 %
4b		96 %
4c		1 %[c]
5a		12 %[c]

5b		41 %[c]
6a		100 %
6b		65 %
9a		100 %
9b		94 %
9c		100 %
9d		100 %
9e		100 %
9f		97 %

9g		100 %
9h		100 %
10a		$IC_{50} = 71 \pm 10\ \mu mol\ L^{-1}$
10b		95 %
10c		$IC_{50} = 13 \pm 2\ \mu mol\ L^{-1}$
10d		100 %
10e		$IC_{50} = 6 \pm 1\ \mu mol\ L^{-1}$
10f		100 %
10g		83 %
10h		100 %

11a		98 %
11b		100 %

[a] Final concentration of the iCP in the assays was 0.2 nmol L^{-1}.

[b] Residual activity (RA) and IC_{50} values are means from at least three independent determinations. Standard errors for RAs were < 15 %.

[c] IC_{50} values could not be determined due to the very poor solubility of compounds in the assay buffer.

Biochemical evaluation

The synthesized compounds were first evaluated for their relative inhibition of β5i activity using Suc-LLVY-AMC as a fluorogenic substrate. The data were calculated as the residual activities (RAs) of β5i in the presence of 100 μmol L^{-1} of each compound. Only compounds that showed notable inhibition (> 20 %) and good solubility in the assay buffer were further characterized by determining their IC_{50} values, with the others deemed as not active (Table I).

Based on the data given in Table I, the structural features for effective inhibition of the β5i subunit of iCP can be deduced. Regardless of the warhead used, the biphenyl derivatives **3–6** showed no inhibition of β5i activity. In addition, these compounds suffered from poor solubility rendering them inadequate for both the proper characterization of inhibition kinetics and for further medicinal chemistry follow-up. The distal phenyl ring was therefore replaced with morpholine in a series of compounds **9–11**. Among these, the acrylamide-based inhibitors **10** proved to be the most promising since three compounds (**10a**, **10c**, **10e**) showed β5i inhibition with IC_{50} values in the low micromolar range. Interestingly, the methylene bridge between the piperidine and the phenyl ring seemed important for inhibitory activity as observed when comparing compounds **10a** (IC_{50} = 71 ± 10 μmol L^{-1}) *vs.* **10b** (RA = 95 %), **10c** (IC_{50} = 13 ± 2 μmol L^{-1}) *vs.* **10d** (RA = 100 %), and **10e** (IC_{50} = 6 ± 1 μmol L^{-1}) *vs.* **10f** (RA = 100 %). Possibly, the carbonyl group at this position resulted in unfavorable interactions within the active site. These observations were in line with our previous studies (32, 42, 43) and research by others (44) in the field of iCP inhibitors, which showed that small structural changes within a given compound class can lead to significant changes in both the β5i inhibition and the subunit selectivity. As the next step in the evaluation of inhibitory characteristics of compounds **10a**, **10c**, and **10e**, we assayed them against other catalytically active subunits of both cCP and iCP (Table II). Surprisingly, we discovered that all compounds almost equipotently inhibited the β1i subunit of the iCP, as well as β1 and β5 subunits of the cCP. Among the three compounds, **10e** was demonstrated to be the most potent as it inhibited all four subunits with IC_{50} values in a single-digit micromolar range (Table II).

Table II. Inhibitory potencies of selected compounds against other subunits (β2i and β1i) of the human iCP and against all subunits (β5, β2, β1) of the human cCP[a]

Compd.	β5i IC$_{50}$ (μmol L^{-1})[c]	β2i RA (%)[b,c]	β1i)[c] IC$_{50}$ (μmol L^{-1})[c]	β5 IC$_{50}$ (μmol L^{-1})[c]	β2 RA (%)[b,c]	β1 IC$_{50}$ (μmol L^{-1})[c]
10a	71 ± 10	100	44 ± 13	38 ± 8	71	16 ± 8
10c	13 ± 2	100	52 ± 12	25 ± 8	81	17 ± 2
10e	6 ± 1	70	9 ± 2	4 ± 0	51	3 ± 1

[a] Final concentrations of the cCP and iCP in the assays were 0.8 nmol L^{-1} and 0.2 nmol L^{-1}, resp.

[b] For β2i and β2 subunits, RAs were measured in the presence of 100 μmol L^{-1} of each compound.

[c] IC$_{50}$ and residual activity (RA) are means from at least three independent determinations. Standard errors for RAs were < 15 %.

*Table III. Determination of the IC$_{50}$ shift for **10e** for the inhibition of β5i and β5 activities without or with 30 min pre-incubation*

Pre-incubation (min)	IC$_{50}$ for β5i (μmol L^{-1})a	IC$_{50}$ for β5 (μmol L^{-1})a
0	7 ± 2	6 ± 2
30	6 ± 1	4 ± 0

[a] IC$_{50}$ values are means from at least three independent determinations.

Because compound **10e** contained an acrylamide moiety, we checked whether this molecule showed time-dependent inhibition of either β5i or β5 subunit using the IC$_{50}$ shift assay (Table III). The IC$_{50}$ values on both proteasome subunits without 30 min pre-incubation of **10e** and the enzyme remained almost exactly the same indicating that this acrylamide-based inhibitor **10e** was not inhibiting β5 subunits of cCP or iCP in an irreversible manner. Although the acrylamide warhead has been successfully used in covalent inhibitors very often, the absence of the covalent interaction with our compounds is most probably due to the mispositioning of the electrophilic carbon of **10e** and the oxygen atom of catalytic Thr1 (in β5i and β5) or Cys48 (within the active site of β5i) (40, 41). It should be noted that such an electrophilic group that is not involved in targeted covalent inhibition could be seen as a liability due to possible off-target effects.

CONCLUSIONS

In this study, we aimed to design structurally distinct non-peptidic derivatives without the central psoralen core. Despite initially aiming to prepare iCP-targeting compounds, the biochemical analyses showed that the designed compounds exhibit different profiles of inhibition in comparison with the parent psoralen-based compounds. Three acrylamide-based derivatives, *i.e.*, **10a**, **10c**, and **10e**, showed inhibition of (immuno)proteasome subunits in the low micromolar range making them suitable for further cell-based evaluations, which are currently underway in our labs. In addition, we plan to further explore

the chemical space of these compounds by replacing morpholine with other saturated heterocycles, such as piperazine. We believe that amino-substituted *N*-arylpiperidinyl--based compounds represent very solid starting hits for further medicinal chemistry optimization towards inhibitors selective for different subunits of cCP and iCP.

Abbreviations, acronyms, symbols. – Ac-PAL-AMC – acetyl-Pro-Ala-Leu-7-amino-4-methylcoumarin; Boc-LRR-AMC – *t*-butyloxycarbonyl-Leu-Arg-Arg-7-amino-4-methylcoumarin; CHOMP – chemical heuristic for optimal molecular pieces; cCP – constitutive proteasome; CP, 20S – core particle; iCP – immunoproteasome; NEAT – novel and electronically-equivalent aromatic template; RA – residual activity; SAR – structure-activity relationship, Suc-LLVY-AMC – succinyl-Leu-Leu--Val-Tyr-7-amino-4-methylcoumarin; UPS – ubiquitin-proteasome system; Z-LLE-AMC – benzyloxy-carbonyl-Leu-Leu-Glu-7-amino-4-methylcoumarin.

Conflict of interest. – The authors declare no competing financial interest in connection with this manuscript.

Supplementary data. – In the supplementary file, detailed synthetic procedures and spectroscopic analyses of all compounds described in the manuscript are available.

Authors contributions. – Conceptualization, A.O., S.G., and I.S.; methodology, M.J., A.B., A.M., Š.P., and J.V.; analysis, A.O. and I.S.; biochemical measurements, M.G..; funding acquisition, M.G., S.G., I.M.R.; writing, original draft preparation, A.O. and I.S.; writing, review and editing, I.S.

All authors have read and agreed to the published version of the manuscript.

REFERENCES

1. R. Raynes, L. C. D. Pomatto and K. J. A. Davies, Degradation of oxidized proteins by the proteasome: Distinguishing between the 20S, 26S, and immunoproteasome proteolytic pathways, *Mol. Aspects Med.* **50** (2016) 41–55; https://doi.org/10.1016/j.mam.2016.05.001

2. I. Sahu and M. H. Glickman, Proteasome in action: substrate degradation by the 26S proteasome, *Biochem. Soc. Trans.* **49**(2) (2021) 629–644; https://doi.org/10.1042/BST20200382

3. D. Voges, P. Zwickl and W. Baumeister, The 26S proteasome: a molecular machine designed for controlled proteolysis, *Annu. Rev. Biochem.* **68** (1999) 1015–1068; https://doi.org/10.1146/annurev.biochem.68.1.1015

4. G. A. Collins and A. L. Goldberg, The logic of the 26S proteasome, *Cell* **169** (2017) 792–806; https://doi.org/10.1016/j.cell.2017.04.023

5. J. A. M. Bard, E. A. Goodall, E. R. Greene, E. Jonsson, K. C. Dong and A. Martin, Structure and function of the 26S proteasome, *Annu. Rev. Biochem.* **87** (2018) 697–724; https://doi.org/10.1146/annurev-biochem-062917-011931

6. F. Türker, E. K. Cook and S. S. Margolis, The proteasome and its role in the nervous system, *Cell Chem. Biol.* **28** (2021) 903–917; https://doi.org/10.1016/j.chembiol.2021.04.003

7. S. A. Bhat, Z. Vasi, R. Adhikari, A. Gudur, A. Ali, L. Jiang, R. Ferguson, D. Liang and S. Kuchay, Ubiquitin proteasome system in immune regulation and therapeutics, *Curr. Opin. Pharmacol.* **67** (2022) Article ID 102310; https://doi.org/10.1016/j.coph.2022.102310

8. L. A. Passmore and D. Barford, Getting into position: the catalytic mechanisms of protein ubiquitylation, *Biochem. J.* **379**(3) (2004) 513–525; https://doi.org/10.1042/BJ20040198

9. S. H. Lecker, A. L. Goldberg and W. E. Mitch, Protein degradation by the ubiquitin–proteasome pathway in normal and disease states, *J. Am. Soc. Nephrol.* **17**(7) (2006) 1807–1819; https://doi.org/10.1681/ASN.2006010083

10. G. Kleiger and T. Mayor, Perilous journey: a tour of the ubiquitin-proteasome system, *Trends Cell Biol.* **24**(6) (2014) 352–359; https://doi.org/10.1016/j.tcb.2013.12.003

11. J. Adams, The proteasome: structure, function, and role in the cell, *Cancer Treat. Rev.* **29** (2003) 3–9; https://doi.org/10.1016/S0305-7372(03)00081-1

12. M. Groettrup, C. J. Kirk and M. Basler, Proteasomes in immune cells: more than peptide producers?, *Nat. Rev. Immunol.* **10** (2010) 73–78; https://doi.org/10.1038/nri2687

13. L. Bedford, S. Paine, P. W. Sheppard, R. J. Mayer and J. Roelofs, Assembly, structure, and function of the 26S proteasome, *Trends Cell Biol.* **20**(7) (2010) 391–401; https://doi.org/10.1016/j.tcb.2010.03.007

14. L. Budenholzer, C. L. Cheng, Y. Li and M. Hochstrasser, Proteasome structure and assembly, *J. Mol. Biol.* **429**(22) (2017) 3500–3524; https://doi.org/10.1016/j.jmb.2017.05.027

15. T. A. Thibaudeau and D. M. Smith, A practical review of proteasome pharmacology, *Pharmacol. Rev.* **71**(2) (2019) 170–197; https://doi.org/10.1124/pr.117.015370

16. E. Ogorevc, E. S. Schiffrer, I. Sosič and S. Gobec, A patent review of immunoproteasome inhibitors, *Expert Opin. Ther. Pat.* **28**(7) (2018) 517–540; https://doi.org/10.1080/13543776.2018.1484904

17. M. Groettrup, S. Khan, K. Schwarz and G. Schmidtke, Interferon-γ inducible exchanges of 20S proteasome active site subunits: Why?, *Biochimie* **83**(3–4) (2001) 367–372; https://doi.org/10.1016/S0300-9084(01)01251-2

18. G. Kaur and S. Batra, Emerging role of immunoproteasomes in pathophysiology, *Immunol. Cell Biol.* **94**(9) (2016) 812–820; https://doi.org/10.1038/icb.2016.50

19. A. Mani and E. P. Gelmann, The ubiquitin-proteasome pathway and its role in cancer, *J. Clin. Oncol.* **23**(21) (2005) 4776–4789; https://doi.org/10.1200/JCO.2005.05.081

20. D. J. Kuhn and R. Z. Orlowski, The immunoproteasome as a target in hematologic malignancies, *Semin. Hematol.* **49**(3) (2012) 258–262; https://doi.org/10.1053/j.seminhematol.2012.04.003

21. M. Schmidt and D. Finley, Regulation of proteasome activity in health and disease, *Biochim. Biophys. Acta BBA – Mol. Cell Res.* **1843**(1) (2014) 13–25; https://doi.org/10.1016/j.bbamcr.2013.08.012

22. J. E. Park, Z. Miller, Y. Jun, W. Lee and K. B. Kim, Next-generation proteasome inhibitors for cancer therapy, *Transl. Res.* **198** (2018) 1–16; https://doi.org/10.1016/j.trsl.2018.03.002

23. V. T. de M. Hungria, E. de Q. Crusoé, R. I. Bittencourt, A. Maiolino, R. J. P. Magalhães, J. do N. Sobrinho, J. V. Pinto, R. C. Fortes, E. de S. Moreira and P. Y. Tanaka, New proteasome inhibitors in the treatment of multiple myeloma, *Hematol. Transfus. Cell Ther.* **41**(1) (2019) 76–83; https://doi.org/10.1016/j.htct.2018.07.003

24. E. M. Huber and M. Groll, Inhibitors for the immuno- and constitutive proteasome: current and future trends in drug development, *Angew. Chem. Int. Ed.* **51**(35) (2012) 8708–8720; https://doi.org/10.1002/anie.201201616

25. A. F. Kisselev and M. Groettrup, Subunit specific inhibitors of proteasomes and their potential for immunomodulation, *Curr. Opin. Chem. Biol.* **23** (2014) 16–22; https://doi.org/10.1016/j.cbpa.2014.08.012

26. P. M. Cromm and C. M. Crews, The proteasome in modern drug discovery: second life of a highly valuable drug target, *ACS Cent. Sci.* **3** (2017) 830–838; https://doi.org/10.1021/acscentsci.7b00252

27. B. L. Zerfas, M. E. Maresh and D. J. Trader, The immunoproteasome: an emerging target in cancer and autoimmune and neurological disorders, *J. Med. Chem.* **63**(5) (2020) 1841–1858; https://doi.org/10.1021/acs.jmedchem.9b01226

28. R. Ettari, M. Zappalà, S. Grasso, C. Musolino, V. Innao and A. Allegra, Immunoproteasome-selective and non-selective inhibitors: A promising approach for the treatment of multiple myeloma, *Pharmacol. Ther.* **182** (2018) 176–192; https://doi.org/10.1016/j.pharmthera.2017.09.001

29. D. J. Sherman and J. Li, Proteasome inhibitors: harnessing proteostasis to combat disease, *Molecules* **25**(3) (2020) Article ID 671 (30 pages); https://doi.org/10.3390/molecules25030671

30. E. M. Huber and M. Groll, A nut for every bolt: subunit-selective inhibitors of the immunoproteasome and their therapeutic potential, *Cells* **10**(8) (2021) Article ID 1929 (21 pages); https://doi.org/10.3390/cells10081929

31. G. R. Tundo, P. Cascio, D. Milardi, A. M. Santoro, G. Graziani, P. M. Lacal, A. Bocedi, F. Oddone, M. Parravano, A. Coletta, M. Coletta and D. Sbardella, Targeting immunoproteasome in neurodegeneration: A glance to the future, *Pharmacol. Ther.* **241** (2023) Article ID 108329; https://doi.org/10.1016/j.pharmthera.2022.108329

32. I. Sosič, M. Gobec, B. Brus, D. Knez, M. Živec, J. Konc, S. Lešnik, M. Ogrizek, A. Obreza, D. Žigon, D. Janežič, I. Mlinarič-Raščan and S. Gobec, Nonpeptidic selective inhibitors of the chymotrypsin-like (β5i) subunit of the immunoproteasome, *Angew. Chem. Int. Ed.* **55**(19) (2016) 5745–5748; https://doi.org/10.1002/anie.201600190

33. E. S. Schiffrer, I. Sosič, A. Šterman, J. Mravljak, I. M. Raščan, S. Gobec and M. Gobec, A focused structure-activity relationship study of psoralen-based immunoproteasome inhibitors, *MedChemComm* **10** (2019) 1958–1965; https://doi.org/10.1039/C9MD00365G

34. E. S. Schiffrer, M. Proj, M. Gobec, L. Rejc, A. Šterman, J. Mravljak, S. Gobec and I. Sosič, Synthesis and biochemical evaluation of warhead-decorated psoralens as (immuno)proteasome inhibitors, *Molecules* **26**(2) (2021) Article ID 356 (18 pages); https://doi.org/10.3390/molecules26020356

35. A. P. Bento, A. Gaulton, A. Hersey, L. J. Bellis, J. Chambers, M. Davies, F. A. Krüger, Y. Light, L. Mak, S. McGlinchey, M. Nowotka, G. Papadatos, R. Santos and J. P. Overington, The ChEMBL bioactivity database: an update, *Nucleic Acids Res.* **42** (2014) D1083–D1090; https://doi.org/10.1093/nar/gkt1031

36. L.-H. Wang, A. Evers, P. Monecke and T. Naumann, Ligand based lead generation – considering chemical accessibility in rescaffolding approaches via BROOD, *J. Cheminf.* **4**(Suppl. 1) (2012) Article ID O20 (1 page); https://doi.org/10.1186/1758-2946-4-S1-O20

37. B. J. Neves, R. V. Bueno, R. C. Braga and C. H. Andrade, Discovery of new potential hits of *Plasmodium falciparum* enoyl-ACP reductase through ligand- and structure-based drug design approaches, *Bioorg. Med. Chem. Lett.* **23**(8) (2013) 2436–2441; https://doi.org/10.1016/j.bmcl.2013.02.006

38. A. Obreza, K. Grabrijan, S. Kadić, F. J. de L. Garrido, I. Sosič, S. Gobec and M. Jukič, Chlorocarbonylsulfenyl chloride cyclizations towards piperidin-3-yl-oxathiazol-2-ones as potential covalent inhibitors of threonine proteases, *Acta Chim. Slov.* **64**(4) (2017) 771–781; https://doi.org/10.17344/acsi.2017.3883

39. A. P. Hill and R. J. Young, Getting physical in drug discovery: a contemporary perspective on solubility and hydrophobicity, *Drug Discov. Today* **15** (15–16) (2010) 648–655; https://doi.org/10.1016/j.drudis.2010.05.016

40. E. M. Huber, M. Basler, R. Schwab, W. Heinemeyer, C. J. Kirk, M. Groettrup and M. Groll, Immuno- and constitutive proteasome crystal structures reveal differences in substrate and inhibitor specificity, *Cell* **148**(4) (2012) 727–738; https://doi.org/10.1016/j.cell.2011.12.030

41. C. Dubiella, H. Cui, M. Gersch, A. J. Brouwer, S. A. Sieber, A. Krüger, R. M. J. Liskamp and M. Groll, selective inhibition of the immunoproteasome by ligand-induced crosslinking of the active site, *Angew. Chem. Int. Ed.* **53**(44) (2014) 11969–11973; https://doi.org/10.1002/anie.201406964

42. L. Kollár, M. Gobec, B. Szilágyi, M. Proj, D. Knez, P. Ábrányi-Balogh, L. Petri, T. Imre, D. Bajusz, G. G. Ferenczy, S. Gobec, G. M. Keserű and I. Sosič, Discovery of selective fragment-sized immunoproteasome inhibitors, *Eur. J. Med. Chem.* **219** (2021) Article ID 113455; https://doi.org/10.1016/j.ejmech.2021.113455

43. L. Kollár, M. Gobec, M. Proj, L. Smrdel, D. Knez, T. Imre, Á. Gömöry, L. Petri, P. Ábrányi-Balogh, D. Csányi, G. G. Ferenczy, S. Gobec, I. Sosič and G. M. Keserű, fragment-sized and bidentate (immuno)proteasome inhibitors derived from cysteine and threonine targeting warheads, *Cells* **10**(12) (2021) Article ID 3431 (19 pages); https://doi.org/10.3390/cells10123431

44. R. Ettari, C. Cerchia, S. Maiorana, M. Guccione, E. Novellino, A. Bitto, S. Grasso, A. Lavecchia and M. Zappalà, development of novel amides as noncovalent inhibitors of immunoproteasomes, *ChemMedChem* **14**(8) (2019) 842–852; https://doi.org/10.1002/cmdc.201900028